

Comparison of Computational Fluid Dynamics and Experimental Testing of a Centrifugal Pump

Doris STAHLJENIĆ*, Mario KOLAR, Pero RAOS, Hrvoje MEŠTRIĆ

Abstract: The work involved research in the field of fluid dynamics. An actual centrifugal radial pump, NNm 65-315, was used as an example; its parameters were tested and compliance with the design values was determined. Deviations in the pump parameters are permitted within the tolerance limits specified by the ISO 9906 Grade 2 standard. The study focused on comparing the results of experimental tests with those of computer analysis. SolidWorks Flow Simulation 2017 was used for the computer analysis, while two pumps of the same type were used for experimental testing. The aim of the paper is to demonstrate the accuracy and reliability of the results obtained from computer analysis.

Keywords: centrifugal pump; computational fluid dynamics (CFD); experimental testing

1 INTRODUCTION

Computational fluid dynamics (CFD) has become a fundamental methodology for the numerical simulation of fluid flows, as it provides engineers and researchers with a reliable approach to investigate and interpret complex fluid dynamics phenomena [1, 2].

CFD is an applied science that predicts fluid flow, heat or mass transfer, and chemical reactions. The results are obtained by solving mathematical equations that represent physical laws. The aim of computer analyses is to reduce the costs and time invested, which are inevitable during experimental tests [3].

CFD provides researchers and engineers with advanced tools to accurately simulate and predict fluid flow phenomena under various operating conditions, facilitating the design of more efficient systems and enabling comprehensive product performance optimisation [4]. CFD is often applied to complex geometries and integrated into the construction process [5]. It is a practical tool that enables you to simulate and calculate various fluid situations. The initial investment is significant, but it does not exceed the costs of experimental testing. The main expense is purchasing a software licence and training the users.

Advantages of computer analysis over experimental testing:

1. Reduced cost and time for prototype development
2. Ability to study systems under difficult-to-control conditions or where experiments are infeasible
3. Ability to study systems under hazardous conditions
4. Continuous repetition of tests
5. Rapid modification of input parameters
6. Simultaneous acquisition of multiple types of results

Computational analysis can process large amounts of data quickly without the added cost of experimental testing. For this reason, it is often used to optimise product performance [6].

The experiment is considered the most important phase of research, and the virtual model must be validated with experimental data, as the simulation is valuable only if it reflects real results [7]. The process of mesh generation in CFD is extremely important, but it requires significant user involvement to ensure reliable and accurate

simulations [8]. As a guideline for mesh generation, it must be adequately fine to ensure an adequate resolution for the main flow characteristics and geometrical structures [9].

The precision of calculation analysis results depends on the number of cells in the network. A larger number of cells yields more reliable results. The fineness or coarseness of the network affects both the reliability of the results and the analysis time required [10].

Optimum networks achieve satisfactory precision with reasonable computation time. The optimal networks are non-uniform, combining finer and coarser divisions in different areas. Finer divisions are used where there are abrupt changes in geometric shapes, while coarser divisions are applied in regions with less significant or more gradual changes. Mesh generation is a fundamental factor in the accuracy and reliability of CFD simulations, as the quality and resolution of the computational grid directly affect the fidelity of numerical predictions and the overall success of the analysis [11]. The user determines the fineness of the network, as there is no universal rule for its definition - only guidelines to help achieve optimal tuning. This highlights how experience with CFD programmes and user expertise influence the accuracy of the results. In addition to numerical data, computer analysis also provides animations to display dynamic results.

Disadvantages of computer analysis arise from incorrect assumptions and inaccurately set input parameters [12]. Errors are caused by human influence. This leads to the presence of errors that may sometimes be negligible, but in some cases have a significant negative impact [13]. To work with complex systems and obtain more precise results, more powerful computers are required. Upon completion of the analysis, the user judges the validity of the results.

Determining the reliability of the CFD numerical simulation method is considered a key problem in the field of research [14]. The precision and accuracy of the final results obtained through computer analysis can be demonstrated only by comparison with experimental testing. Therefore, this work is dedicated to demonstrating the reliability and relevance of the results obtained by computer analysis.

The subject of the test, on which the capability of computer analysis was assessed, is shown in Fig. 1. The

trajectories illustrate the distribution of fluid flow rate through the pump.

The results obtained from computer analysis were compared with those from experimental tests on two identical centrifugal radial pumps, NNm 65-315.

The conclusion, based on the collected data from all tests and the referenced literature, is presented at the end of the paper.

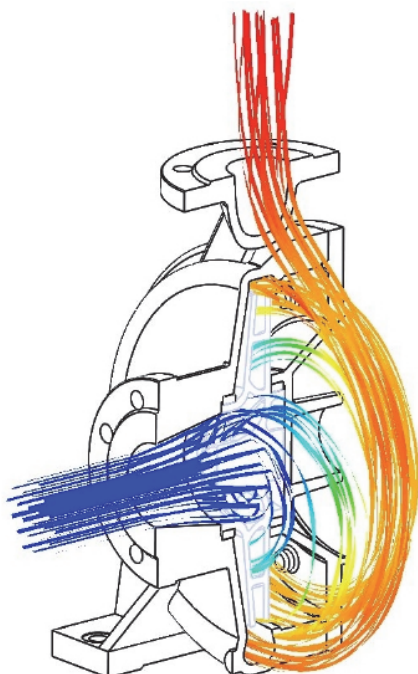


Figure 1 Illustration of the fluid velocity distribution in a centrifugal pump [16]

2 ANALYSED CENTRIFUGAL PUMP

2.1 Selecting the Type of Centrifugal Pump

During experimental and computer testing, a horizontal single-stage centrifugal pump was used. The pump was designed in accordance with DIN 24255 or EN 733.

Table 1 Characteristic features of a centrifugal pump [15]

Horizontal single-stage centrifugal pump			
Characteristic features of the pump	Physical quantity	Value	Unit of measurement
Flow rate	Q	1-100	l/s
Supply height	H	50-90	m
Pressure	p	16	bar
The temperature of the transported fluid	t	10-140	°C
Revolutions per minute	n_{max}	2900	o/min

In Tab. 1, the values of the basic parameters required for the intended application are provided for the selected pump. According to the requirements of specific parameters, it is necessary to select an appropriate type and size of pump.

Each pump type covers a broad operating range, even though it is designed for an optimum point, particularly within the range where efficiency approaches its maximum value.

According to Fig. 2 the diagram shows the areas of supply height H (ordinate) and flow rate Q (abscissa) that certain types and sizes of pumps can achieve at a specific number of revolutions ($n = 24,2$ rps).

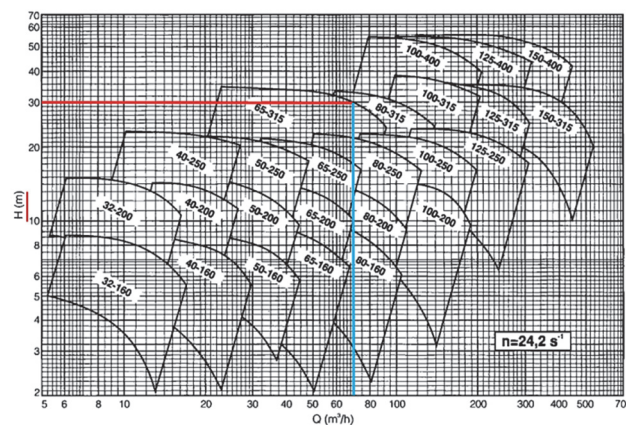


Figure 2 Centrifugal pump supply range [15]

When selecting a pump for the given case, it is necessary for it to meet the flow criterion Q of 70 m³/h (blue line) and the supply head criterion H of 30 m (red line). By intersecting the lines for easier visualisation, it is evident that the 65-315 type pump satisfies these criteria. The first value in the label 65-315 represents the diameter of the pressure nozzle at the outlet, expressed in millimetres ($d = 65$ mm). The second value in the designation 65-315 indicates the outer diameter of the rotor, also expressed in millimetres ($d_2 = 315$ mm) [16].

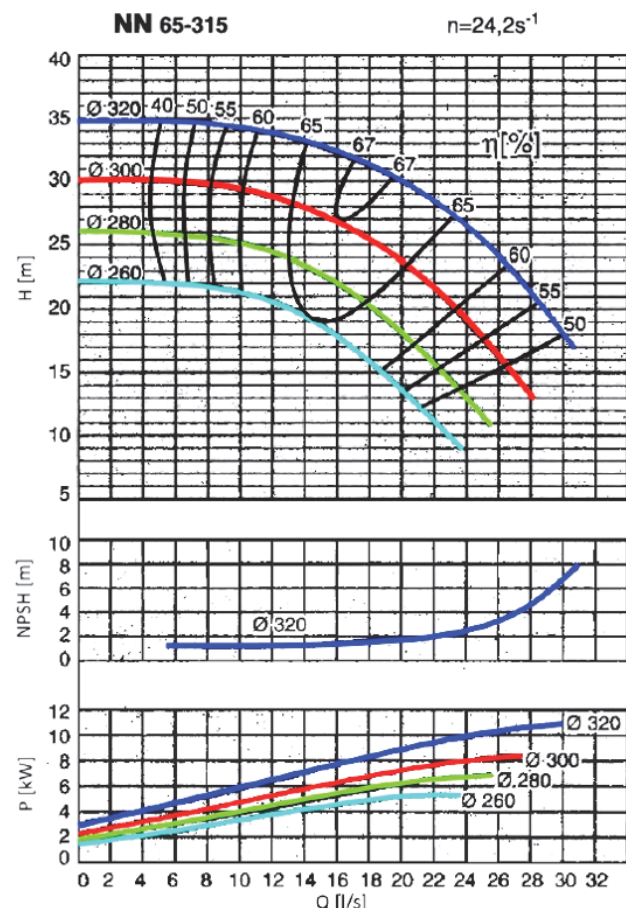


Figure 3 Diagram of basic characteristics of pump type NN 65-315 [15]

All remaining data can be obtained from the diagrams in Fig. 3. From the first diagram, the efficiency η [%] is determined by the intersection of the supply height H and flow rate Q lines. In the second diagram, with the known flow rate Q , the net positive suction head $NPSH$ [m] is

obtained. The third diagram shows the power P [kW] as a function of the flow rate Q [l/s]. The diameter dimensions of the installed rotor are indicated next to each curve, referring to the outer diameter d_2 , which varies according to requirements. Identical diameters are highlighted in the same colours in each diagram for easier identification.

2.2 Pump NNm 65-315

Fig. 4 shows the selected type of centrifugal pump that meets the criteria for flow rate Q and delivery height H . The first position indicates the pump, the second the electric motor, the third the clutch, and the fourth the stand.

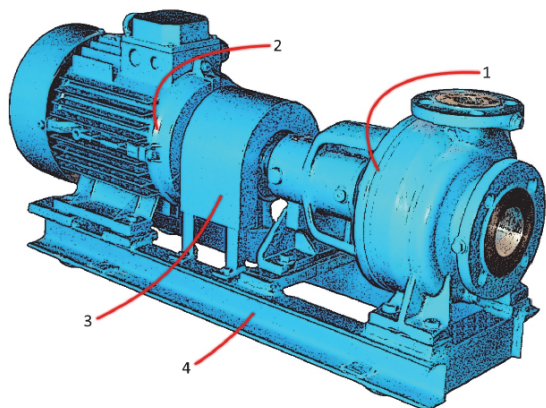


Figure 4 Pump NNm 65-315 [15]

The pump and motor components are connected in an assembly by a flexible coupling and mounted on the same base plate. Rotating parts such as rotors and shafts can be removed from the intake and pressure pipelines without disassembly. Maintenance is simplified by the elastic coupling, which allows the pump to be dismantled without moving the pump housing or motor. The pump is suitable for a wide range of applications, including transferring water containing small amounts of solid particles, seawater, and clean heated or cold water. It is commonly used in energy and industrial plants where low pressure is present, as well as in many water supply systems.

The pump can be exchanged with pumps from other manufacturers, as guaranteed by the standard to which it was designed. The standard specifies the designs of connections and bases. The hydraulic characteristics depend on the quality of the production process [17].

3 EXPERIMENTAL TESTING

Experimental research was conducted under controlled conditions to prevent the influence of external factors that could lead to erroneous results [18]. The accuracy of the test results depends on the methods used and the controlled conditions under which the test is conducted. Simulating the conditions in which the pump will operate in the real environment as realistically as possible yields more precise results. For this reason, this experimental test was conducted at the test station.

3.1 Experimental Methodology

The test was carried out on a test station that is verified and approved for operation at the company Croatia Pumpe Nova d.o.o. The company complies with ISO 9001 and ISO

14001 standards, was founded in 1949, and has been operating continuously since then. It is engaged in the development, manufacturing, and overhaul of pumps and pump assemblies, primarily centrifugal types. It also holds additional certificates, for example in the field of welding.

On the specific test station, there is a number of additional devices and instruments that serve as redundancy or enable more precise measurements. All instruments undergo regular inspection and possess the appropriate certifications. The pump test sheet represents the original test documentation and was officially delivered to the customer of the pump assembly, confirming the credibility of the measurements performed.

3.2 Examination Station

The test station is a device used to assess the operation of the pump under controlled conditions [19]. It contains essential components which allow various types of pumps to be correctly installed and prepared for testing in accordance with regulations. These components include valves, pipelines, couplings, electric motors, drive machines, and others.

A certain amount of liquid stored in reservoirs is also required for testing the pump. Plain water is mainly used, but other media transported by the pump may be used if necessary.

Measuring techniques and equipment for fluid flow measurement play a major role in the testing process. There are several methods of flow testing, and in recent times, more devices directly provide output values suitable for computer processing. These are implemented in all areas of measurement, improving plant digitalisation, process monitoring and data handling.

Measuring equipment uses precise manometers for pressure measurement and vacuum gauges for vacuum measurement. These enable indirect measurement of delivery heads and suction capacity of the pump. The torque measuring device measures power, and together with the device that measures rotational speed, provides information about the mechanical power at the pump coupling (P_2). The same data can be obtained by measuring current and voltage; in this case, the efficiency of the electric motor should also be considered. The value obtained in this way is the total installed power required for the operation of the pump unit (P_1).

In tests where the dimensions of the model differ from the actual size, it is necessary to scale the actual values according to the definitions of mutual relationships.

3.3 Examination Procedure

3.3.1 Preparation for Examination

The pump is mounted in the assembly with the electric motor, which is positioned on a properly secured base. The entire assembly is placed on the test station. Pressure and suction pipelines are connected to the pump, along with all other elements required for initiating and conducting measurements. Before starting the test, it is necessary to be familiar with the standards governing the test, select an appropriate pipeline, assess risks, and implement protection and safety measures. During the test, electrical components are energised, while the rest of the equipment is subjected to high pressure.

All air must be evacuated from the system, as the pump operates only when completely filled with fluid. Once all

The measurement points represent each individual intermediate phase of valve opening and closing V_i .

Fig. 7 graphically presents the data generated from the database using the test sheet shown in Fig. 6.

Fig. 8 shows the changes in characteristics after recalculating the data of the outer diameter of the rotor d_2 .

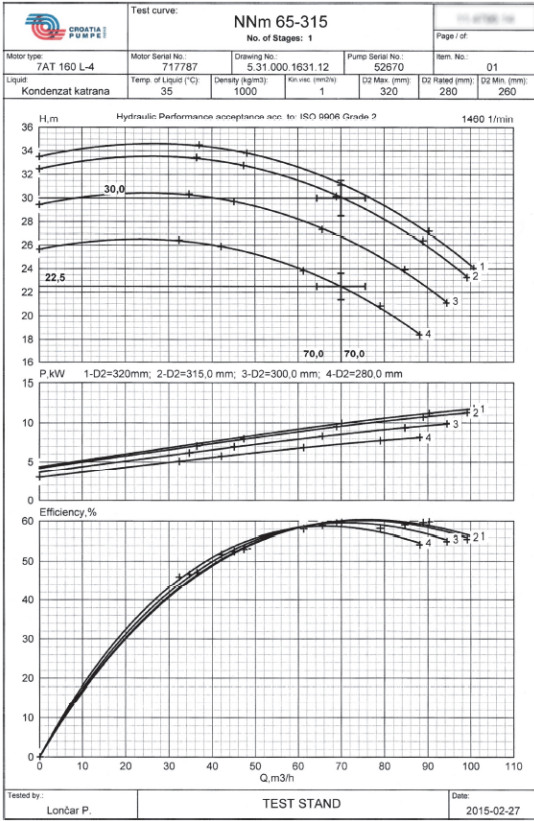


Figure 8 Diagram of pump characteristics comparison variants 1 [16]

Fig. 9 and Fig. 10 show the test data of the second pump. Fig. 9 shows the data that was filled in during the test in a table.

Fig. 10 shows graphically the data generated according to the database from the test sheet in Fig. 9.

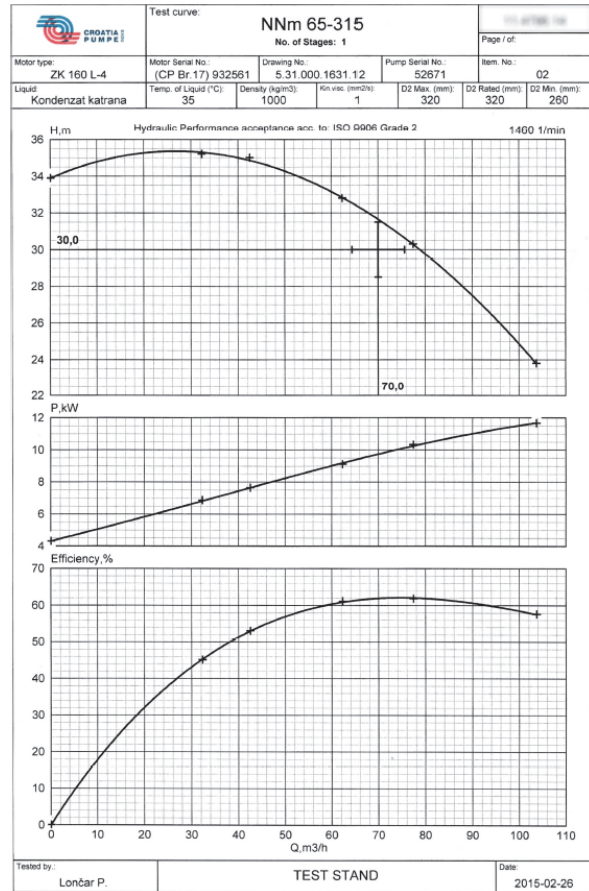


Figure 10 Diagram of characteristics of pump 2 according to the test sheet [16]

Mjerenje/Measuring		Godina/Year	
1		2015.	
Gradnja/Year		02	
UGOVORENO / CONTRACTED			
Q=	70 m³/h	U _s	1000 kg/m³
H=	30 m	T=	35 °C
NPSH=	3,0 m	pH=	8,5-9
n=	1460 1/min	v=	1 mm²/s
ρ=	9,8 kg/m³	Medij/Liquid	Kondenzat katrana
η=	58,2 %	d=	320 mm
isp.medij / Meas.Liquid: Voda/Water			
ρ=	1000 kg/m³	DN _s =	80 mm
pv=	0,0233 bar	DN _n =	65 mm
Mjerne točke/Measuring points			
SNAGA / POWER			
KAPACITET / CAPACITY			
VISINA / TOTAL HEAD			
M.BR. OBR. / KONST. BR. OBR. / SPEED CALCULATE			
Mjerenje param. El. Motora / Measuring of engine with			
Kupac/Client			
Kućićta/Casing			
Tlačna proba / Hydraulic tested			
Datum/Date			
Mjesto ispitivanja/Locality			
Preuzeo/Verify			
Datum/Date			
Potpis/Signature			

Figure 9 Test sheet - pump 2 [16]

At the beginning of the test sheet, information is provided about the contracted or designed values, the measuring devices used, and the electric motor, while details about the protocols are found at the end of the sheet. In the middle section of the test sheet, there is a measurement scheme, which lists the parameters used for measurement:

- Power P
- Capacity - flow Q
- Supply height H
- Parameters with a constant number of revolutions n .

All parameters were measured in several measuring points and the remaining values were interpolated over the measuring points, based on which diagrams were obtained as a result (Fig. 7; Fig. 10).

In the first section of the test sheet, the installed power P_1 is analysed in the table marked as $P_{mot/eng}$. In the same category, data on the electric current consumption/according to the voltage U is presented. By considering the efficiency of the electric motor and the $\cos\phi$ parameter, the total power is calculated using Eq. (1), [16]:

$$P_1 = \frac{U \cdot I \cdot \cos\phi}{\eta_{mot}} \quad (1)$$

If the engine efficiency η_{mot} is not included in the equation, the power P_2 is obtained by calculation, which is marked P_{pum} in the table of the test sheet.

The second section "Capacity" of the test sheet includes information on the achieved flow in a certain unit of time. The time period in which a certain volume was filled was measured using the volumetric vessel.

Eq. (2) represents the velocity energy in the measurement of the delivery height. Through flow Q and factor k , the second part of the expression, i.e. data not shown in the table of the test sheet, is presented.

$$\Delta c^2 \cdot \frac{1}{2 \cdot g} = k \cdot Q^2 \quad (2)$$

The third column "Height" shows the value y , which indicates the geodetic pressure difference between the measurement point and the measuring sensors. Parameters h_t and h_s show the measured pressure values on the suction and pressure flanges of the pump. The parameters H are used to record the pressure values and the delivery height. In order to define the total value, it is necessary to add up the other parameters in the column with pressure differences. During calculations, it is necessary to use the same measurement units [16].

According to Eq. (3), the fact that the density of water at 20 °C is 998,2 kg/m³ was taken into account. With that in mind, a pressure of one bar represents a difference in height of approximately 10,2 meters. The stated values are taken as a reference for calculations with the amount of supply [16].

$$Q = n \cdot V_s \quad (3)$$

4 COMPUTATIONAL FLUID DYNAMICS

4.1 Preparation of Data for Processing

4.1.1 Construction of a Three-Dimensional Model

The reference data source is a two-dimensional drawing of the pump assembly. The design was based on a classic calculation and a diagram showing the pump's characteristics. For this analysis, the required input data for the test sample is a three-dimensional model of the pump assembly. Accordingly, a three-dimensional model of all components is created and then assembled into a single assembly [16].

To achieve the same conditions as in the experimental approach, it is necessary to construct a 3D model that is almost identical to the design of the actual product [20]. Particular attention is given to the spiral casing and the rotor, as these are key parts to analyse. The initial data have a direct impact on the results. More precise results are obtained by ensuring a greater similarity between the data of the real product and the model [16].

Fig. 11 illustrates the construction of the rotor, progressing from a two-dimensional drawing to a three-dimensional model. The right side of the image presents a simplified sketch of the blades without the rotor's upper cover. The pump's parameters largely depend on the rotor. The upper and lower covers of the rotor are constructed using simple shapes [16].

Blades are crucial components, and their design receives significant attention. The housing spiral and rotor blades are created using the "Surface" technique in the CAD programme. By applying various commands, it is possible to generate complex free-form shapes. To better represent the geometric shape of the blades, the lower part of the image shows the rotor without a section of the upper cover.

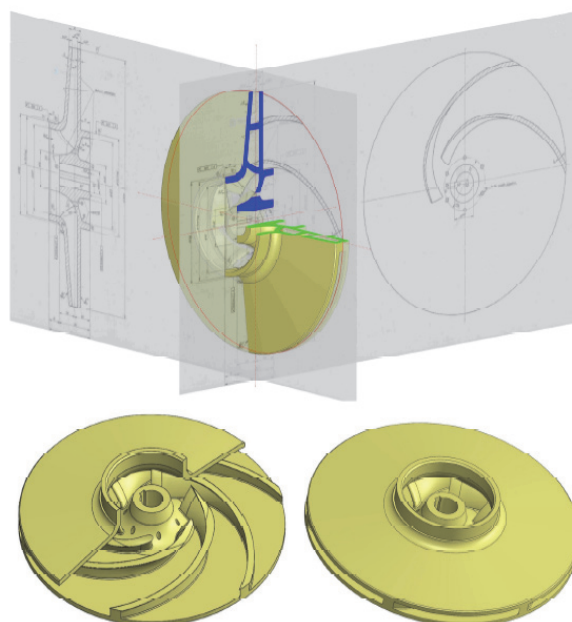


Figure 11 Construction of the rotor from the workshop drawing into a three-dimensional model [16]

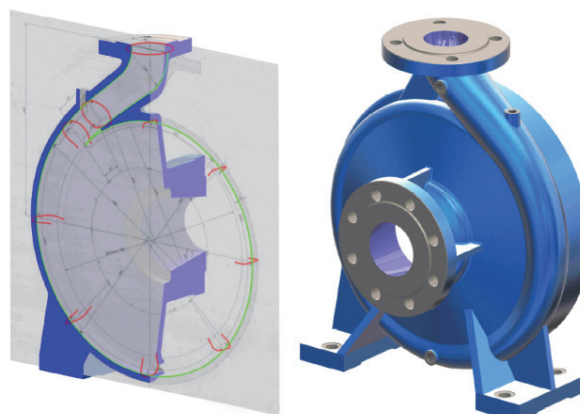


Figure 12 Construction of the spiral pump housing [16]

Fig. 12 shows a section where the constantly changing characteristic shapes of the cross-section are marked in red. The green line indicates the closed spiral of the casing's hydraulic channel formed by the cross-sections. In the right part of the image, a three-dimensional model of the pump housing is shown [16].

4.1.2 Optimization of the Three-Dimensional Model

According to Fig. 13, a three-dimensional model of the pump assembly is visible. The rotor and the spiral casing are the main parts that together with other secondary parts form a functional product. Clutch, stand, electric motor shown in Fig. 4 are not modelled. The reason for this is that they are not necessary for computational testing as opposed to experimental testing.

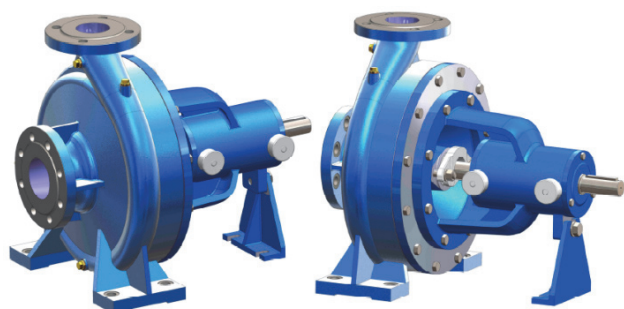


Figure 13 Three-dimensional model of the pump assembly NNm 65-315 [16]

During analyses to check the hydraulic characteristics, the entire assembly is not always shown, but only the key parts. Accordingly, during the analysis, the parts that direct the fluid through the pump, that is, that transmit certain energy to the fluid, are included. The parts that are included in the analyses are the rotor and the spiral casing with the cover.

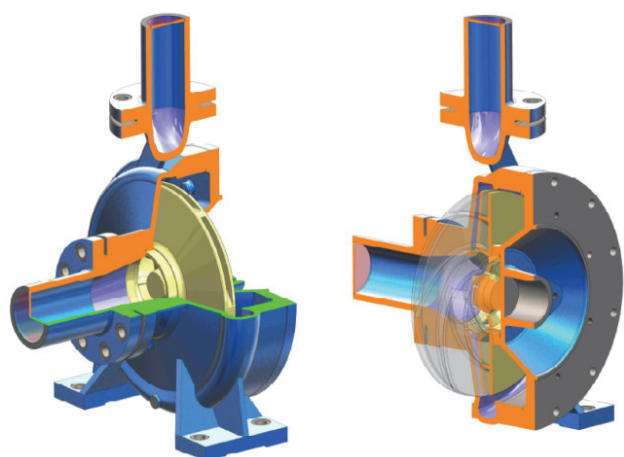


Figure 14 Display of pump parts included in the analysis [16]

In order to ensure mathematically accurate conditions for the development of flow on the pressure and suction side, the initial elements of the pipeline were added, which more realistically simulate the drain and supply of fluid. Fig. 14 shows the caps at the beginning and end of the pipeline, which are set as boundary conditions in the analysis [16].

Parts that do not disrupt the fluid flow are omitted from the 3D model for easier creation of the model mesh. Excluded parts include: nuts, washers, screws and gauge fittings.

4.1.3 Corrected Value Data

Tab. 2 shows the summarized test results from the measurement sheets for ease of monitoring. Values 5-8 are required for the calculation of the Δp_{tot} data. Y is the correction factor for setting the measuring instruments in relation to the centre of the pump. At the end of the computer analysis, the parameter y was added to the total pressure difference in the pump Δp_{tot} . The data Δp_{geo} was neglected in the computer analysis as well as in the experimental test. The parameters Δp_{geo} and y do not represent the same relationships.

Tab. 3 shows the corrected values that are used in computer analysis. Given that the distribution of the speed

energy difference at the pump's outlet and inlet is not known, it is not possible to use total pressures for the input data [16].

It follows that they apply values of known static pressures, while other pressure values are obtained through simulation.

Table 2 Summary of the pump test sheet 1[16]

PUMP 1 - RESULTS FROM THE TEST STATION						
Measuring points	1	2	3	4	5	6
1 n - number of revolutions / min^{-1}	1491	1485	1483	1480	1478	1477
2 P_1 - power / kW	5,2	8,6	9,7	11,5	12,9	13,6
3 P_2 - power / kW	4,68	7,74	8,73	10,35	11,61	12,24
4 Q - flow rate / m^3/h	0,0	37,7	48,8	71,0	91,4	101,9
5 Δp_{dyn} - velocity energy / m	0,00	0,29	0,48	1,02	1,69	2,09
6 y - height of measuring devices / m	0,84	0,84	0,84	0,84	0,84	0,84
7 $p_{\text{stat-out}}$ - outlet pressure / bar	3,28	3,30	3,17	2,74	2,10	1,70
8 $p_{\text{stat-in}}$ - inlet pressure / bar	-0,06	-0,09	-0,12	-0,21	-0,39	-0,42
9 Δp_{tot} - pressure difference / bar	3,42	3,50	3,42	3,13	2,74	2,41
10 H - supply height / m	34,9	35,7	34,9	32,0	27,9	24,6

Table 3 Prepared pump 1 data for computer analysis [16]

PUMP 1 - DATA FOR CFD ANALYSIS						
Measuring points	1	2	3	4	5	6
1 n - number of revolutions / min^{-1}	1491	1485	1483	1480	1478	1477
2 P_1 - power / kW	5,2	8,6	9,7	11,5	12,9	13,6
3 P_2 - power / kW	4,68	7,74	8,73	10,35	11,61	12,24
4 Q - flow rate / m^3/h	0,0	37,7	48,8	71,0	91,4	101,9
5 $p_{\text{stat-out}}$ - outlet pressure / bar	4,28	4,30	4,17	3,74	3,10	2,70
6 $p_{\text{stat-in}}$ - inlet pressure / bar	0,94	0,91	0,88	0,79	0,61	0,58
7 Δp_{stat} - pressure difference / bar	3,34	3,39	3,29	2,95	2,49	2,12

The amount of atmospheric pressure was added to the data Δp_{stat} and $p_{\text{stat-in}}$ so that the values are expressed in absolute amounts.

It was agreed that the amount of the flow parameter at the inlet and the amount of the static pressure parameter at the pump outlet were taken as the boundary conditions. In this way, the simulation of the valve closing as during the experimental test was achieved.

4.2 CFD Settings and Approach

In this chapter, the complete numerical approach used in the CFD analysis is presented. The numerical assumptions that influence the stability and accuracy of the simulation are defined. The aim of the chapter is to clearly outline the methodology to ensure the repeatability and transparency of the obtained results.

4.2.1 Convergence Criteria

SolidWorks Flow Simulation, despite the numerous options, functions, and methods it offers, is certainly not the most comprehensive software for solving CFD problems. The basic operating principle of the solver is based on the finite volume method (FVM), Cartesian numerical meshing, an iterative CFD solver, and a

modified $k-\varepsilon$ turbulence model. Along with all the advantages it provides, the software also has certain limitations.

The available options for selecting convergence criteria include several approaches. In this case, the Goal Convergence method was chosen, whereby all defined and assigned goals converge through the required number of iterations until the convergence conditions are met. All parameters of the convergence conditions were left at default settings, except for the Volume Flow Rate parameter, for which a tolerance of 3% was manually set.

Among the other available convergence criteria, there are the options:

- Physical Time (the time interval of pump operation that the simulation must process is defined)
- Iterations (the exact or expected number of iterations in the calculation is determined)
- Travels (the number of passes the simulation must perform is defined)
- Calculation Time (the total calculation time for a single simulation is defined).

4.2.2 Mesh Independence Analysis

Network independence, at least in the context of this work, represents a key factor in obtaining high-quality and reliable results. The testing was carried out through a larger number of repeated simulations while maintaining the same input parameters (Inlet Volume Flow and Static Pressure), along with other general settings, while the only variable was the size of the mesh.

There are currently five different scenarios in the SolidWorks document, with the mesh size increasing incrementally by 100000 control volumes per scenario. This means that in the final case the mesh contains 500000 control volumes.

By analysing all parameters between individual mesh sizes (especially the required, i.e., "Goal" results), it can be concluded that the set of results between the 100000 and 400000-volume meshes deviates on average by around 20 %, while some parameters deviate by up to 30%. The mesh-independence analysis above 400 000 control volumes shows differences of only 1-2%, which no longer represent a significant influence on the final result.

The parameter measuring turbulence was excluded from the analysis, since the initial input value is not sufficiently relevant, and therefore the deviations in the result are expectedly larger. This parameter affects energy-related aspects to a greater extent, and hydraulic performance to a lesser extent.

A summary of deviations between the 100 000 and 400 000 meshes is as follows:

- Flow: ~ 0,07% (negligible)
- Velocity: ~ 6%
- Pressure (local IN): ~ 30%, ΔP : ~ 17%
- Torque: ~ 18,5%.

These are values that must be taken into account when designing new systems in practice. Errors of such magnitude would be unacceptable in real applications, but the goal here was to provide insight into CFD simulations and explain certain phenomena that occur in fluid mechanics.

4.2.3 Impact of Numerical Parameters on Simulation Results

Mesh independence is a key factor and a prerequisite for the reliability and relevance of the obtained results. A certain level of imprecision is undoubtedly present in the work.

The base mesh used in the analysis contains 100000 discretized control volumes. Such a mesh is sufficient for an overview and conceptual analysis of the case. However, for concrete requirements and design validation, this parameter is one of the most important for achieving acceptable and reliable solutions.

4.2.4 The Turbulence Model

In the SolidWorks Flow Simulation software, it is possible to select the mode of observing the flow. In the simulation, the analysis was set to include both laminar and turbulent flow conditions (although the flow in the actual pump is certainly turbulent), and this result is shown in the generated reports for each mesh size. Turbulence in SolidWorks Flow Simulation is modelled exclusively using the modified $k-\varepsilon$ model, which as such does not offer significant control capabilities, representing one of the major limitations of the software.

In the simulation settings, under General Settings, within Flow Characteristics → Flow Type, the option *Laminar and Turbulent* was selected. The setting was left at its default values defined by the I_t and L_t factors: $I_t = 2\%$ / $L_t = 0,0042$ m

However, it is more likely that the actual turbulence intensity at the pump inlet is at least 5-10 % (or higher). Despite the importance of this parameter, it should be noted that it was not a specific subject of direct comparison in the analysis. In the simulation, additional so-called inlet and outlet pipe extensions were added to the pump inlet and outlet in order to stabilise the flow and reduce the influence of initially unfavourable flow formation directly at the pump suction.

4.2.5 Numerical Settings

In the SolidWorks Flow Simulation software, in addition to the basic settings in the *General Settings* menu that define the type of analysis - where the options *Fluid Flow*, *Time-dependent*, and *Rotation Type* set to *Local Region Sliding* were selected in the *Physical Features* section - there are three additional groups of parameters.

In *Fluid Type*, the medium *Water* was selected. In *Wall Conditions*, surface roughness was not taken into account, and the default *Wall Thermal Condition* was left as *Adiabatic Wall*.

In *Initial Conditions*, within the thermodynamic parameters, the external pressure was set to 1,01325 bar, and the ambient and water temperature to 19 °C.

4.3 Data Processing and Analysis Procedure Configuration

At the beginning of the programme, the project name is defined and the measurement units are set. The SI system of measurement units is established. Additionally, the units of measurement are harmonised with those on the test sheet for easier comparison.

The next step is to select the "Internal" type of analysis. This type was chosen because, during the analysis of the pump, solid boundaries (casing) are defined for the fluid under observation.

In the existing database, it is possible to choose from many gases and liquids. For this analysis, water was selected as the working fluid.

Below is the determination of the wall of the observed system. The adiabatic properties of the walls were set, assuming there are no thermal changes in the system. The initial conditions at the start of the analysis were determined. Thermodynamic parameters of pressure at 101325 Pa and temperature at 293,2 K were set.

The next step determined the area of the computational domain shown in Fig. 15 (left). For the internal type of analysis, the largest area covered by the test object (pump) was automatically selected.

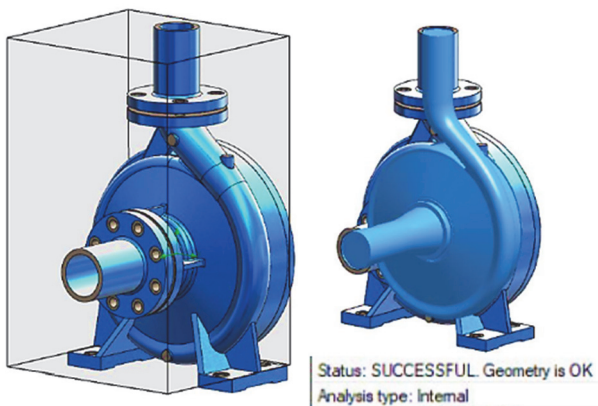


Figure 15 Computational domain selection and geometry verification [16]

To start the simulation, the volume impermeability condition within the observation domain must be satisfied. In Fig. 15 (right), the impermeable volume inside the pump is marked in blue. By checking the geometry in the lower part, the successful placement of the geometry is confirmed [16].

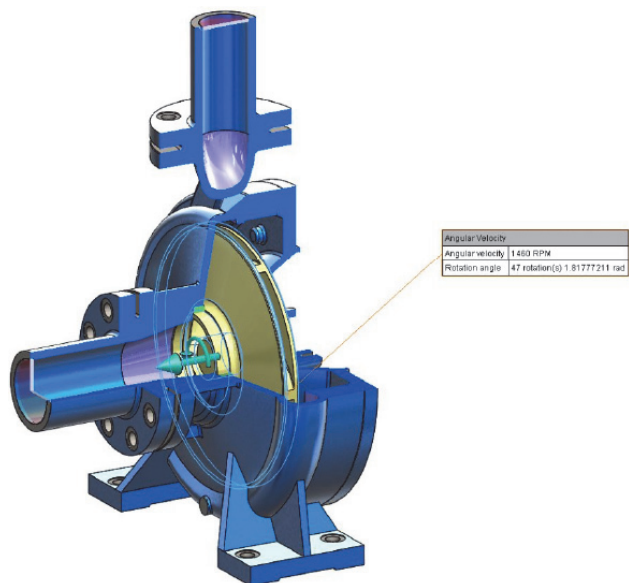


Figure 16 Region and speed of rotation [16]

Fig. 16 shows the selected region of rotation and the speed parameter in the amount of 1460 rpm.

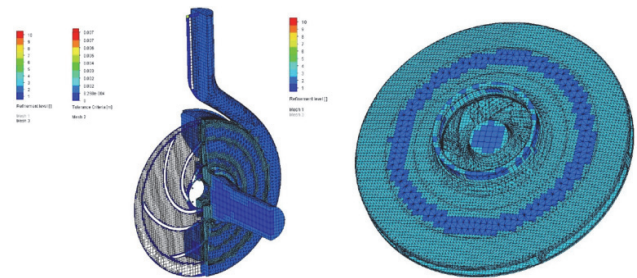


Figure 17 Display of created networks [16]

Fig. 17 (left) shows the global mesh, while Fig. 17 (right) shows the local and moving mesh on the rotor. A finer mesh is applied to the rotor compared to the rest of the model to obtain more accurate results [16].

Boundary conditions are defined for specific observed areas. When testing a pump, the boundary conditions correspond to all fluid inlets and outlets with their respective characteristics. At all measuring points, the values of the flow rate Q were set, while the values of the static pressures $p_{stat-out}$ were set at the pump outlet.

In the next step, the goals are defined, specifying the parameters to be monitored during the simulation and used to evaluate the solutions. Goals such as volume flow, pressures, speed, and others are set.

After entering all the data and criteria, the calculation begins. A total of 98667 control volumes with 1073 iterations were processed, and the results obtained were further analysed [16].

4.4 Presentation of Computer Analysis Results

Fig. 18 shows the distribution of the average pressure distribution in two planes.

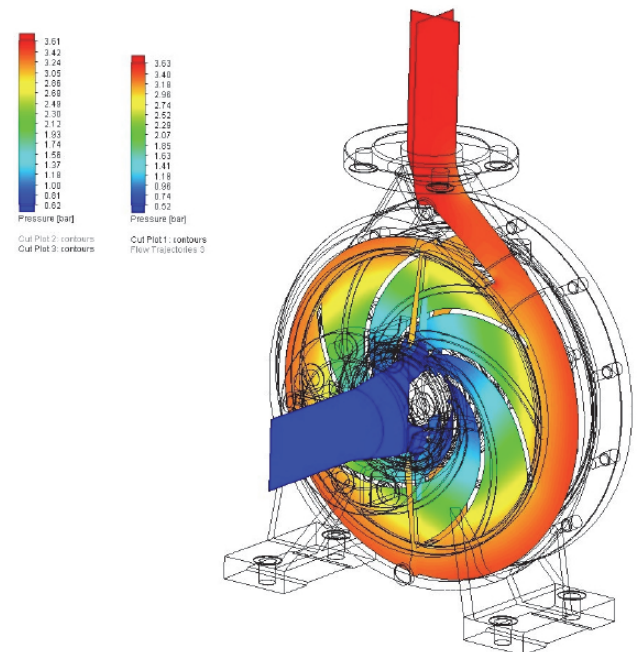


Figure 18 Distribution of pressure distribution in the pump [16]

Fig. 19 represents the distribution of fluid velocity in the pump with particle movement lines [16].

Fig. 20 shows the trajectories of particles in space, with colours indicating the relative pressure distribution within the pump. The pump inlet pressures are shown in blue,

while the pump outlet pressures are shown in red. This illustrates how the pressure increases gradually from the inlet to the outlet of the pump. Considering this pressure movement, it is clear how the pump performs its primary function by increasing the pressure in the system [16].

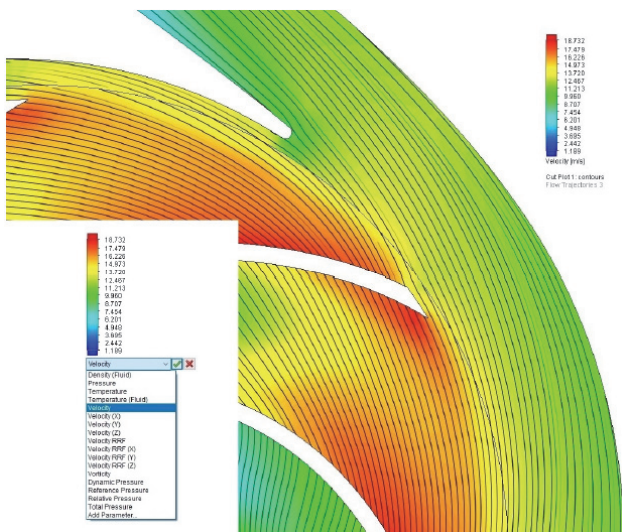


Figure 19 Velocity distribution [16]

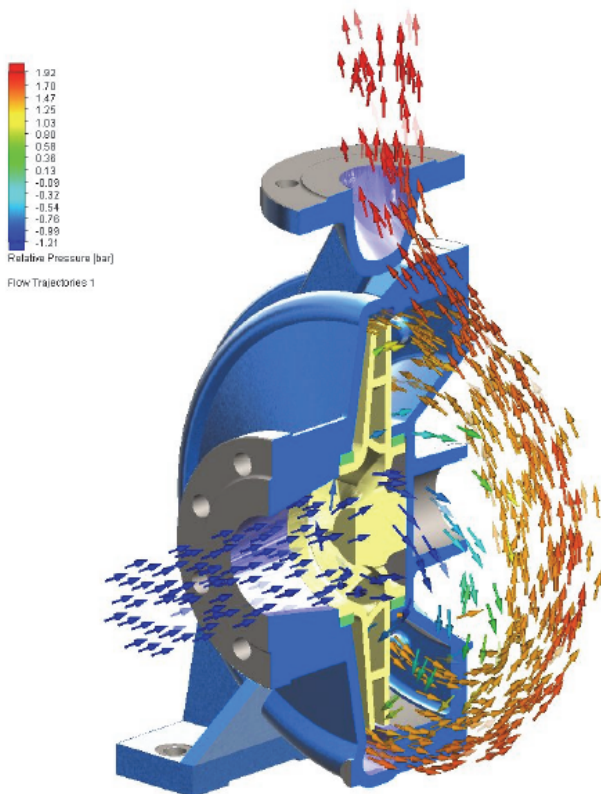


Figure 20 Dynamic display of trajectories [16]

In addition to visual data, numerical data was also delivered and analysed.

Tab. 4 presents the monitored parameters with their minimum, average and maximum values. It includes data on the criteria and accuracy of the results, as well as information on the successfully completed process. Negative values for flow rate and torque were recorded according to the defined coordinate system.

In addition to the tabular values, comparative data are also shown in diagrams [16].

Table 4 Tabular results of computer analysis [16]

Goal Name	Unit	Value	Averaged Value	Minimum Value	Maximum Value	Progress [%]	Use In Convergence	Delta	Criteria
SG Volume Flow Rate 1 OUT	[m ³ /h]	-71,01326	-71,00805	-71,02123	-70,99749	100	Yes	0,000760192	1,832173715
SG Av Static Pressure 1 IN	[bar]	0,70734	0,74873	0,67430	0,85932	100	Yes	0,00488412	1,832173715
SG Av Static Pressure 2 OUT	[bar]	3,74000	3,74000	3,74000	3,74000	100	Yes	0	3,74E-08
SG Av Total Pressure 1 IN	[bar]	0,78593	0,82729	0,75287	0,93788	100	Yes	0,00488412	1,832173715
SG Av Total Pressure 2 OUT	[bar]	3,92986	3,92976	3,92947	3,92995	100	Yes	0,000486318	0,000489071
SG Av Dynamic Pressure 1 IN	[bar]	0,07856	0,07856	0,07856	0,07856	100	Yes	0	7,85648E-10
SG Av Dynamic Pressure 2 OUT	[bar]	0,18986	0,18976	0,18947	0,18995	100	Yes	0,000486318	0,000489071
SG Av Velocity 1 IN	[m/s]	3,94227	3,94227	3,94227	3,94227	100	Yes	2,66454E-15	3,94227E-08
SG Av Velocity 1 OUT	[m/s]	6,07827	6,07716	6,07418	6,07901	100	Yes	0,004825687	0,006500325
SG Torque (Z) 1	[N*m]	-52,98150	-53,08657	-53,35781	-52,85993	100	Yes	0,026124316	25,93956332
d Ptot	[bar]	3,22595	3,18447	3,07399	3,25892	100	Yes	0,005561926	1,832173845

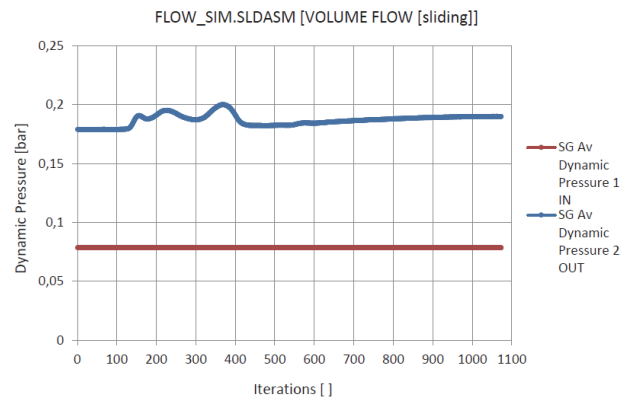


Figure 21 Dynamic pressure change diagram during the calculation process [16]

Fig. 21 shows the dynamic pressure change diagram at the pump inlet and outlet during the calculation.

All obtained results of the computer analysis are compared with the experimental test in the next chapter.

5 COMPARISON OF RESULTS OF COMPUTER AND EXPERIMENTAL ANALYSIS

The data obtained from the experimental measurement for pump 1 are presented in Tab. 2, and the necessary data for creating the *H-Q* diagram are summarized in Tab. 5. These are not the same data according to which the previous pump diagrams were created (Fig. 7; Fig. 8; Fig. 10). The data from Tab. 5 was obtained through the actual number of revolutions achieved at the test station [16].

The numbers in the legend are also linked to the number of the corresponding table.

Table 5 Pump 1 data for *H-Q* diagram according to test station results [16]

Pump 1 - results from test station No. (1)		
Measuring points	Flow rate <i>Q</i> / m ³ /h	Supply height <i>H</i> / m
1	0,0	34,9
2	37,7	35,7
3	48,8	34,9
4	71,0	32,0
5	91,4	27,9
6	101,9	24,6

Analogous to the data from Tab. 5, Tab. 6 presents the data obtained by computer analysis.

In accordance with the data from Tab. 5 and Tab. 6, *H-Q* curves were created, which are shown in the diagram from Fig. 22.

Solid lines with highlighted points indicate curves created by measurement at the test station and computer analysis. Dashed lines indicate additional curves interpolated over a second degree polynomial. Given that this is how flow and delivery height data are normally described in practice for pumps [16].

Table 6 Pump 1 data for H - Q diagram according to computer analysis results [16]

Pump 1 - results of computer analysis No. (2)		
Measuring points	Flow rate Q / m ³ /h	Supply height H / m
1	0,0	35,3
2	37,7	35,9
3	48,8	35,3
4	71,0	32,4
5	91,4	25,8
6	101,9	22,4

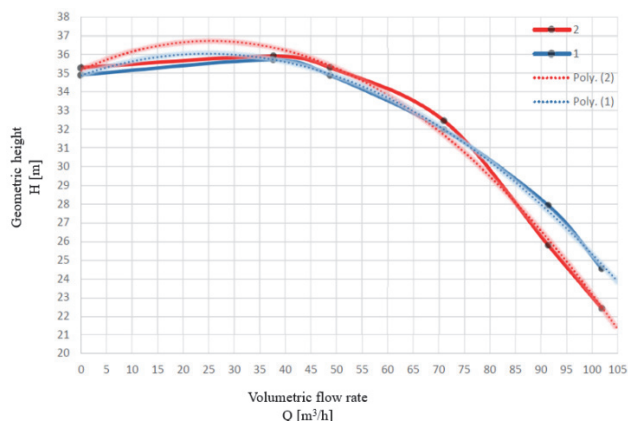


Figure 22 H - Q characteristics of real and virtual measurement [16]

In accordance with the data from Tab. 5 and Tab. 6, H - Q curves created by interpolation of the measured points via the second degree polynomial were created, which are shown in the diagram from Fig. 23.

The test curve for pump 2, which includes data with realistically achieved revolutions, has not been added to the diagram because the characteristics of the pumps can only be compared at the same or constant numbers of revolutions.

In practice, during the experimental procedure for testing pumps, some parameters fluctuate. These fluctuations affect the consistency of result observation. Oscillations are reflected in changes in the network voltage and mainly influence the number of revolutions of the pump. Under real conditions, such oscillations are accepted, but when determining the universal parameters of the pump, it is necessary to adjust the revolutions to a constant value [16].

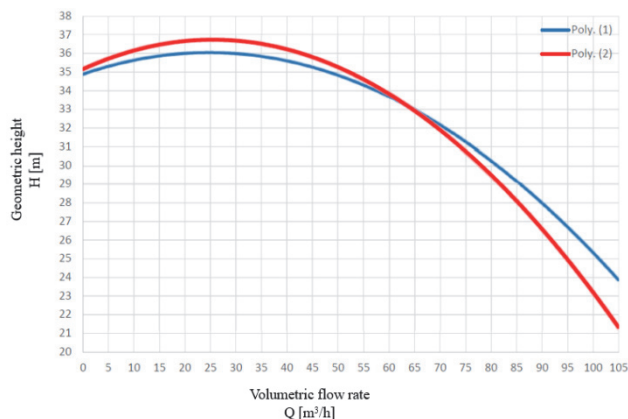


Figure 23 H - Q characteristics expressed by polynomials of the second degree [16]

According to the diagram from Fig. 23, the other H - Q diagrams presented in the rest of the paper will be interpreted.

The obtained results from the test sheets according to Fig. 6 and Fig. 9 are adjusted to a constant number of revolutions of 1460 min⁻¹. For each pump, the obtained data are shown in Tab. 7 and Tab. 8. According to the data from the tables, the diagrams in Fig. 7, Fig. 8, Fig. 10 were constructed [16].

Table 7 Pump parameters 1 with a constant number of revolutions [16]

Pump 1 - results from test station No. (1) $n = \text{konst}$		
Measuring points	Flow rate Q / m ³ /h	Supply height H / m
1	0,0	33,5
2	37,0	34,5
3	48,1	33,8
4	70,0	31,1
5	90,3	27,2
6	100,7	24,0

Table 8 Pump parameters 2 with a constant number of revolutions [16]

Pump 2 - results from test station No. (2) $n = \text{konst}$		
Measuring points	Flow rate Q / m ³ /h	Supply height H / m
1	0,0	33,9
2	32,3	35,2
3	42,5	35,0
4	62,3	32,8
5	77,4	30,3
6	103,7	23,8

Tab. 7 and Tab. 8 show data with a constant number of revolutions so that they can be compared correctly through the diagrams.

The data show that the experimental testing did not achieve equal sample sizes. This inequality is even more evident in the diagrams.

The data in Tab. 6 are values selected according to the parameters of the experimental test of pump 1, that is, the data from the measuring points of that test.

The result obtained from the computer analysis must be converted to a constant number of revolutions. This allows for a more accurate comparison of the results.

Table 9 Computer analysis values converted to a constant number of revolutions [16]

Results of computer analysis No. (3) $n = \text{konst}$		
Measuring points	Flow rate Q / m ³ /h	Supply height H / m
1	0,0	33,8
2	37,1	34,7
3	48,1	34,2
4	70,0	31,6
5	90,3	25,2
6	100,7	21,9

The obtained data from Tab. 9 are considered unique regardless of the values taken for the input parameters of the boundary conditions (measuring points) of the computer analysis.

According to the data from Tab. 7, Tab. 8, Tab. 9 the H - Q curves for both pumps and the curve created by computer analysis were created. All data are aligned with a constant number of revolutions.

According to the diagram in Fig. 24, similarities can be observed between curves (1) and (2), which represent the results of the experimental test. The curve (3) was created using computer analysis data. Larger deviations in the form of overlapping with the other two curves are observed [16].

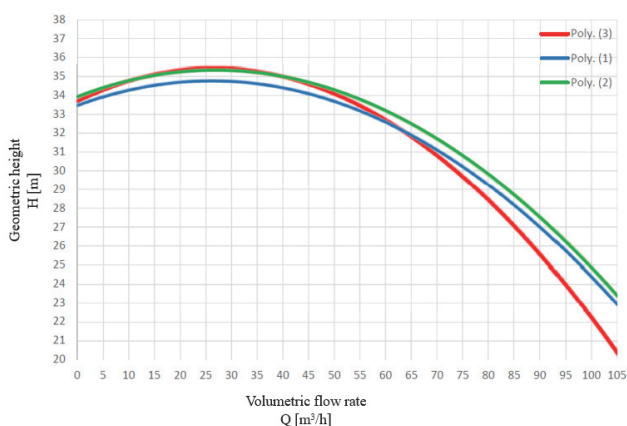


Figure 24 H-Q curves at a constant number of revolutions [16]

According to Fig. 3, a diagram of the characteristics of the NNm 65-315 pump was obtained at a speed of 24,2 s⁻¹. After reading the values from the diagram and calculation analysis with a constant number of revolutions (1460 min⁻¹) obtained values shown in Tab. 10.

Table 10 Data for the H-Q diagram of the pump NNm 65-315 according to the nominal diagram [16]

Data of nominal values No. (4) n = konst		
Measuring points	Flow rate Q / m ³ /h	Supply height H / m
1	0,0	34,4
2	37,2	34,8
3	48,3	34,0
4	70,4	30,8
5	90,5	25,5
6	102,6	21,2

The result of the nominal values and computer analysis is shown in the diagram in Fig. 25 through the H-Q characteristics from Tab. 9 and Tab. 10. As shown in the diagram in Fig. 25, an almost identical overlapping of curves (3) and (4) was achieved. Curve (3) is the same as the curve from Fig. 24. Curve (4) was made using the data from Tab. 10 [16].

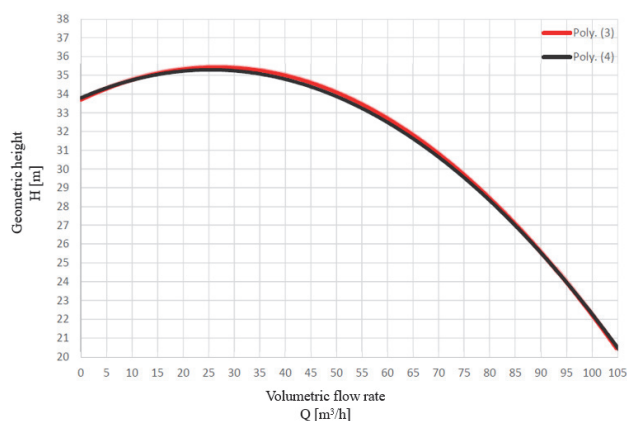


Figure 25 Result of computer analysis and nominal values of the pump [16]

For a simpler comparison, the data of pump characteristics, computer analysis and nominal values of the NNm 65-315 pump are combined in Tab. 11.

On the same diagram shown in Fig. 26, all H-Q curves compatible with the data from Tab. 11 are combined.

Table 11 Data for all analysed curves of the H-Q diagram [16]

	Pump 1 - results from test station	Pump 2 - results from test station	Data of nominal values	Results of computer

Measuring points	No. (1) n = konst		No. (2) n = konst		No. (3) n = konst		analysis No. (4) n = konst	
	Q / m ³ /h	H / m	Q / m ³ /h	H / m	Q / m ³ /h	H / m	Q / m ³ /h	H / m
1	0,0	33,5	0,0	33,9	0,0	33,9	0,0	33,8
2	37,0	34,5	32,3	35,2	37,2	34,8	37,1	34,7
3	48,1	33,8	42,5	35,0	48,3	34,0	48,1	34,2
4	70,0	31,1	62,3	32,8	70,4	30,8	70,0	31,6
5	90,3	27,2	77,4	30,3	90,5	25,5	90,3	25,2
6	100,7	24,0	103,7	23,8	102,6	21,2	100,7	21,9

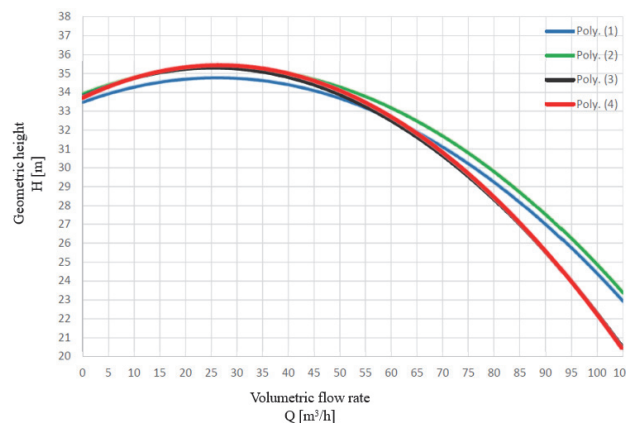


Figure 26 Diagram of all observed H-Q curves [16]

From the diagram in Fig. 26, it is possible to conclude that the curves of pumps (1) and (2) deviate from the curve (3), which represents the nominal value. A certain similarity that is noticeable between the curves of the actually manufactured pumps leads to the conclusion that the rotors (the main influencing elements curves) produced almost identically. The methods and prerequisites present in the rotor processing technology in production lead to differences and thus to the mismatch of curves (1) and (2) with curve (3). The satisfactory overlapping of curve (4) from the computational analysis with curve (3), which is considered as a reference, is noticeable. The data confirmed the reliable and accurate results obtained by the computer analysis process for creating H-Q curves [16].

The hydraulic power P_{hyd} was not measured in the experimental test. The values of the total power of the pump unit P_1 were tested. The hydraulic power values of P_{hyd} were collected by computer analysis.

The relationship between hydraulic forces can be determined according to the expression:

$$P_1 > P_2 > P_{hyd} \tag{4}$$

If only the results are observed and their reliability is not considered, it is evident that the characteristic curves of the actual pumps obtained by measurement on the test station are shown in blue and green. The black line represents the nominal values according to the catalogue data of the manufacturer Croatia Pumpe Nova d.o.o., while the red line shows the results of the CFD analysis. Based on the diagram itself, it can be observed that the highest degree of correspondence is shown by the curves of pumps 1 and 2. There is also a clearly expressed overlap between the nominal value curves and the CFD simulation results. Although such overlap suggests a very good, almost ideal prediction, it may nevertheless be the consequence of an insufficiently dense numerical mesh in the CFD model, i.e.,

an insufficient number of control volumes. The difference between the two tested pumps is relatively small. In the initial part of the diagram, all curves match well, while at higher flow rates the difference between the pump curves and the CFD results with nominal data increases. Such divergence most likely indicates deviations in the geometry of the hydraulic channels of the pump casing and rotor that occurred during the manufacturing process. Imperfections caused by the casting process and subsequent technological preparation and machining operations are possible, which directly affect the hydraulic performance and characteristic of the pump. It is also necessary to take into account the surface roughness, i.e., the quality of the prepared hydraulic channels of the tested pumps.

The power values of P_2 from the nominal diagram of the pump are shown in Tab. 12.

Table 12 Power values P_2 shown from the nominal diagram of the pump [16]

Nominal diagram data No. (1) $n = \text{konst}$		
Measuring points	Flow rate Q / m ³ /h	Supply height H / m
1	0,0	3,3
2	22,0	5,3
3	47,0	7,0
4	65,0	8,4
5	94,0	10,7
6	102,0	10,8

P_{hyd} power data were obtained through computer analysis and are shown in Tab. 13.

Table 13 Hydraulic power data obtained by computer analysis [16]

Results of computer analysis No. (2) $n = \text{konst}$			
Measuring points	Flow rate Q / m ³ /h	Moment M / Nm	Power P_{hyd} / kW
1	0,0	17,8	2,7
2	37,7	37,9	5,8
3	48,8	43,0	6,6
4	71,0	53,0	8,1
5	91,4	61,2	9,4
6	101,9	65,1	9,9

By applying Eq. (5), the power data P_{hyd} shown in Tab. 13 was obtained:

$$P_{\text{hyd}} = M \cdot \omega \tag{5}$$

Eq. (6) for calculating the angular velocity must also be included in the calculation of power P_{hyd} . The equation includes a constant number of revolutions n , which is included in the measurement unit [s⁻¹].

$$\omega = 2 \cdot \pi \cdot n \tag{6}$$

The data obtained by experimental analysis through the measurement of power P_1 on the pump are shown in Tab. 14.

Using the data taken from Tab. 12, Tab. 13, Tab. 14 curves were created and placed in the common power and flow diagram for the NNm 65-315 pump shown in Fig. 27.

Fig. 27 shows the logical and correct relationship between the observed powers P_1 , P_2 and P_{hyd} . The power P_1 is represented by the upper line in the diagram and is clearly the highest power used. Apparently, the power of

P_{hyd} is the smallest amount. The upper line P_1 depends on the efficiency of the drive electric motor [16].

Table 14 Power data P_1 and P_2 for pump 1 [16]

Pump 1 - results from the test station No. (3) $n = \text{konst}$		
Measuring points	Flow rate Q / m ³ /h	Power P_1 / kW
1	0,0	4,9
2	37,0	8,2
3	48,1	9,3
4	70,0	11,0
5	90,3	12,4
6	100,7	13,1

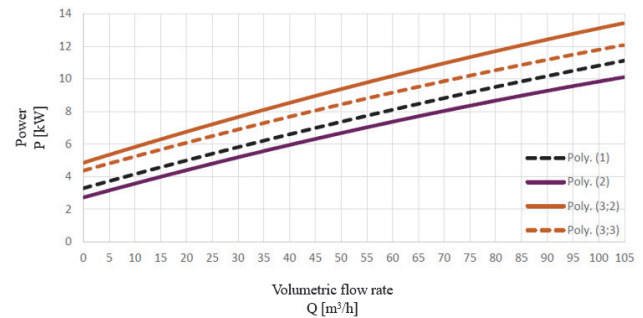


Figure 27 P-Q diagram of all powers in the NNm 65-315 pump [16]

The upper dashed line shows the result obtained from the experimental test, while the lower dashed line shows the nominal values. The upper dashed line and the lower dashed line should overlap for the best case. Therefore, it is possible to conclude that in the real case the pump consumes a little more power compared to the calculation assumption.

Gaps, visible between power curves directly represent losses. They are also connected via the pump efficiency parameter.

The values of the hydraulic or total efficiency of the pump are shown in Tab. 15.

Table 15 Pump efficiency according to computer and experimental analysis [16]

Measuring points	Results of computer analysis No. (1) $n = \text{konst}$					Pump 1 - results from the test station No. (2) $n = \text{konst}$			
	Q / m ³ /h	H / m	P_{hyd} / kW	η_{hyd} / %	η_{tot} / %	Q / m ³ /h	H / m	P_1 / kW	η_{tot} / %
1	0,0	33,8	2,7	0,0	0,0	0,0	33,5	4,4	0,0
2	37,1	34,7	5,8	60,5	47,7	37,1	34,5	7,4	47,4
3	48,1	34,2	6,6	68,1	53,8	48,1	33,8	8,3	53,1
4	70,0	31,6	8,1	74,3	60,6	70,0	31,1	9,9	59,7
5	90,3	25,2	9,4	66,2	55,3	90,3	27,2	11,2	59,8
6	100,7	21,9	9,9	60,5	50,9	100,7	24,0	11,8	55,7

In accordance with Eq. (7), the data for the efficiency η_{tot} shown in Tab. 15 were obtained:

$$\eta_{\text{tot}} = \eta_m \cdot \eta_{\text{hyd}} \cdot 100\% \tag{7}$$

Fig. 28 presents the efficiency diagram of pump 1 based on computer and experimental analyses. Solid lines indicate the differences in total efficiency η_{tot} between computer analysis and experimental testing. The dashed curve represents the hydraulic efficiency η_{hyd} from the computer analysis [16].

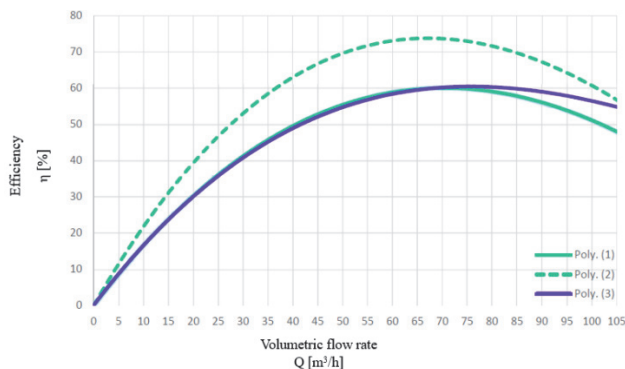


Figure 28 Efficiency diagram of pump 1 according to computer and experimental analysis [16]

The comparison of results is based on the logic and method of data recording used in the test station measurement protocols. The same analogy was applied in the CFD simulation, achieving the highest possible level of consistency and correspondence between the procedures. The dataset from the measurement protocols originates from the application used by the test station, while additional calculated values were included in the CFD simulation. For example, during the setup of the simulation task, a parameter for calculating the maximum torque was added, as well as a formula that automatically computes the pressure difference at the pump inlet and outlet.

The differences between the results obtained under real test station conditions and those from the CFD simulation were not analysed in detail, nor was a full physical interpretation of the observed phenomena. Such an analysis may be the subject of future research.

6 DISCUSSION

Results obtained by computer analysis can provide sufficient accuracy, comparable to experimental testing. The accuracy of these results largely depends on the knowledge and skills of the person performing the computer analysis. At the outset, it is necessary to correctly identify and formulate the fluid flow problem in terms of the relevant physical or chemical phenomena. Key decisions arise when modelling problems in two or three dimensions, controlling the ambient temperature of the analysed system, and considering the influence of pressure changes on air density, among other factors. Modelling requires strong skills, as assumptions are made to reduce complexity to a manageable level while retaining all essential features of the problem.

Achieving accurate results depends on determining the geometry of the domain and designing the mesh. The concepts of convergence and grid independence indicate a favourable outcome. The algorithm for solving the problem is based on iterative methods, which require very small measures of overall conservation of the flow property. By eliminating unnecessary factors according to specific criteria, progress is made towards a converged solution. Choices depend on the particular problem, so there are no unequivocal guidelines for this procedure. Experience contributes to effective system optimisation. In cases of inadequate mesh creation, there is no formal method to evaluate the error.

A mesh independence verification study is the only way to avoid errors caused by an excessively coarse mesh.

This process involves repeating the test with increasing mesh fineness until the results no longer deviate significantly from the previous iteration. This step is a key part of computational analysis. Ultimately, the person conducting the test must assess the validity of the results.

The diagram (Fig. 24) presents the data via $H-Q$ curves at a constant number of revolutions. Curves (1) and (2) represent the results of the experimental test and similarities can be observed. Curve (3) deviates a little more in overlapping than the other two curves and it represents the data obtained by computer analysis.

The diagram (Fig. 25) presents the data through $H-Q$ curves of the nominal value and computer analysis. Curves (3) and (4) achieved an almost identical overlap.

The diagram (Fig. 26) presents the data of all observed $H-Q$ curves. Pump curves (1) and (2) deviate from curve (3), which represents the nominal value. The similarity of the curves (1) and (2) of the actually manufactured pumps results from the fact that the rotors are manufactured almost identically. Incomplete matching of pump curves (1) and (2) with curve (3) results from the fact of preconditions present in rotor processing technology. Superimposing the curve (4) from the computational analysis with the curve (3), which is considered as reference, gives sufficiently approximate results. The data confirm the credibility and accuracy of the results obtained by the computer analysis process for creating $H-Q$ curves.

The diagram (Fig. 27) shows the logical relationship between the observed powers P_1 , P_2 and P_{hyd} . Power P_1 is visibly the largest power used while power P_{hyd} is the smallest amount. The power of P_1 depends on the efficiency of the driving electric motor. Ideally, experimental test results and nominal values should match. In the real case, the pump consumes a little more power compared to the calculation assumption.

The diagram (Fig. 28) shows the efficiency data of pump 1 compared to the experimental test showing total minor deviations. Larger deviations are visible when the flow rate increases from 80 m³/h and higher.

The deviations observed between the experimental test and computer analysis compared to the designed values do not have a significant practical impact. According to the ISO 9906 Grade 2 standard, the pump remains within acceptable tolerances and therefore meets the required criteria. The observed differences occur at the far right of the pump characteristic curve. Due to reduced efficiency and unfavourable conditions, the pump is never operated under these circumstances.

Results obtained from any type of test are subject to measurement errors. In experimental testing, errors may occur when reading values from measuring devices. In computer testing, errors can result from incorrect input data and neglecting network independence. In most cases, such errors are negligible, but in certain situations they can significantly affect the final outcome.

7 CONCLUSION

There is room for more advanced simulations or additional mesh-independence measurements, which is also the main factor influencing the reliability of the results, particularly within the SolidWorks Flow Simulation package. In the work, the compared results

were those obtained from measurements (practical testing and simulation) of the Q - H diagram, power, and efficiency. The simulation additionally included a parameter for calculating the torque [Nm] generated due to the load caused by fluid flow through the pump. Although this value is very important for shaft design, it was not the subject of direct comparison in this work; instead, it served for cross-checking results in the context of mesh-independence evaluation.

Under the defined and presented conditions in the work, primarily referring to the mesh density of 100000 control volumes, the main conclusion is that the analysis shows good convergence of results. The direction and magnitude of deviations in the criteria are acceptable, the physical reliability of the system and the mesh quality are at the limit of acceptability, and the overall result can be considered a good proof-of-concept. It can be concluded that additional mesh-independence verification is required, which can be characterised as the main limitation of this work. Other aspects represent an extension of the observation domain, further research, and additional analyses.

The simulation did not account for thermal conduction, cavitation, gravity, surface roughness, and similar effects. Furthermore, although turbulence was left at default settings - which certainly does not correspond to real conditions - it also contributes to the final result. It should also be noted that even with accurate inlet data for the specific case, the capabilities of SolidWorks Flow Simulation would still be limited due to the use of only one type of turbulence solver and its lower suitability for high-turbulence flow conditions.

The acceptability of results in practice depends on the specific circumstances. Typically, an acceptable error is defined as a percentage deviation affecting the accuracy of the results, and according to the technical literature, it is often considered to be less than 5%. Based on the conducted mesh analysis and validation of results, it can be concluded that the CFD model provides stable and consistent results at a mesh density of ≥ 400000 control volumes. It reliably describes the hydraulic behaviour of the pump and enables the estimation of performance (pressure, torque, efficiency) with acceptable accuracy. The accuracy at 100000 volumes is noticeably lower; with an acceptable error of 5%, the total deviation averages around 15%. Such behaviour indicates the presence of numerical diffusion in the case of a coarse mesh, resulting in overestimation of energy-related quantities. Increasing the mesh density improves the description of boundary layers, vortex structures, and rotor-casing interactions, making the results more physically realistic.

Further research may include evaluating results at mesh sizes of 800000 or even 1.5-2 million control volumes. Such analysis requires significantly longer computation time, depending on available computational resources. For a complete analysis, it would be necessary to run simulations for all six operating points observed on the test station and to include specific turbulence data.

The main goal of the work was to demonstrate, using a specific example of a centrifugal pump, that the results of computer analysis provide accurate, credible, and useful information. The comparison between computer analysis and experimental research produced a positive outcome.

Data from computer analysis were obtained in a much shorter time and at lower research costs. Diagrams graphically display minor deviations in computer analysis compared to experimental research.

According to the ISO 9906 Grade 2 standard, the pump is within the tolerance limits of the design values based on the data from experimental research and computer analysis. Therefore, the NNm 65-315 pump meets the criteria.

Acknowledgements

This research paper was funded by the University of Slavonski Brod through the institutional research project "Improving production process quality through modern technological solutions", financed by the European Union-NextGenerationEU. The views and opinions expressed in this paper are those of the author and do not necessarily reflect the official position of the European Union or the European Commission. Neither the European Union nor the European Commission can be held responsible for them.

8 REFERENCES

- [1] Rahman, M. S., Hazra, S., & Chowdhury, I. A. (2024). Advancing computational fluid dynamics through machine learning: A review of data-driven innovations and applications. *Journal of Fluid Mechanics and Mechanical Design*, 6(2), 42-51. <https://doi.org/10.46610/JFMMD.2024.v06i02.005>
- [2] Madhu, B. P., Sameer, S., Kumar, M. K., & Mani, G. M. (2017). CFD analysis of convergent-divergent and contour nozzle. *International Journal of Mechanical Engineering and Technology*, 8(8), 670-677.
- [3] ANSYS, Inc. (2010). Introduction to the CFD methodology: Customer training material.
- [4] Chowdhury, I. A. (2024). State-of-the-art CFD simulation: A review of techniques, validation methods, and application scenarios. *Journal of Recent Trends in Mechanics*, 9(2), 45-53. <https://doi.org/10.46610/JoRTM.2024.v09i02.005>
- [5] Stern, F., Wilson, R. V., Coleman, H. W., & Paterson, E. G. (1999). Verification and validation of CFD simulations. <https://doi.org/10.21236/ADA458015>
- [6] Versteeg, H. K. & Malalasekera, W. (2007). *An introduction to computational fluid dynamics* (2nd ed.). Pearson Education.
- [7] Sobieski, W. (2013). Relationships between CFD and experimental fluid mechanics. *Technical Sciences*, 16(3), 169-178.
- [8] Cooper Lorsung, C. & Barati Farimani, A. (2023). Mesh deep Q network: A deep reinforcement learning framework for improving meshes in computational fluid dynamics. *AIP Advances*, 13(1), 015026. <https://doi.org/10.1063/5.0138039>
- [9] Tu, J., Yeoh, G.-H., & Liu, C. (2018). *Computational fluid dynamics: a practical approach* (3rd ed.). Butterworth-Heinemann.
- [10] Kathiresan, M., Umamageswari, A., & Subramanian, J. (2020). *Compatibility and accuracy of mesh generation in HyperMesh and CFD simulation with AcuSolve for torque converter*. Technical Report CFD-FEM-09.
- [11] Ibraheem, A. (2021). Evaluating the efficiency of polyhedral mesh elements in solving the problem of the flow around ship's rudder. <https://doi.org/10.21791/IJEMS.2021.2.212021>
- [12] Andreozzi, A., Bianco, N., Musto, M., & Rotondo, G. (2019). Parametric analysis of input data on the CFD fire

- simulation. *Journal of Physics: Conference Series*, 1224(1), 012011. <https://doi.org/10.1088/1742-6596/1224/1/012011>
- [13] Taylor, J. R., Semon, M. D., & Pribram, J. K. (1983). Post-use review: An introduction to error analysis: The study of uncertainties in physical measurements. *American Journal of Physics*, 51(2), 191-192. <https://doi.org/10.1119/1.13309>
- [14] Yang, S. S., Li, D. Y., Kupka, D., Kolonicny, J., & Singh, P. (2024). CFD numerical simulation, verification with experimental results and internal flow analysis of bristle turbines. *Case Studies in Thermal Engineering*, 64, 105436. <https://doi.org/10.1016/j.csite.2024.105436>
- [15] Croatia pumps: Standard pump type NN. https://croatia-pumpe.com/images/pdf_katalozi/brodske_pumpe/NN.pdf
- [16] Kolar, M. (2018). *Computational fluid dynamics and CFD applications in practice*. Master's thesis, Karlovac University of Applied Sciences.
- [17] Ren, Z., Li, D., Qin, Y., Wang, H., Liu, J., & Li, Y. (2023). Correlation between hydraulic loss and characteristic vorticities in a mechanical pump. *Physics of Fluids*, 35(6), 065120. <https://doi.org/10.1063/5.0156118>
- [18] Em, S. (2024). Exploring experimental research: Methodologies, designs, and applications across disciplines. *SSRN Electronic Journal*. <https://doi.org/10.2139/ssrn.4801767>
- [19] Petre Ciuc, P.-O., Mădulărea, R. A., Georgescu, A.-M., Diminescu, M. A., & Georgescu, S.-C. (2019). Experimental test rig designed to analyse pumping station operation controlled by pressure at different key points. *E3S Web of Conferences*, 85, 06001. <https://doi.org/10.1051/e3sconf/20198506001>
- [20] Yang, C., Kang, J., & Eom, D.-S. (2024). Enhancing ToF sensor precision using 3D models and simulation for vision inspection in industrial mobile robots. *Applied Sciences*, 14(11), 4595. <https://doi.org/10.3390/app14114595>

Contact information:

Doris STAVLJENIĆ, MSc. in Mech. Eng., Lecturer
(Corresponding author)
University of Applied Science Zagreb,
Vrbik 8, 10000 Zagreb
E-mail: doris.stavljenic@tvz.hr

Mario KOLAR, MSc. in Mech. Eng.
University of Applied Science Karlovac,
Trg Josipa Jurja Strossmayera 9, 47000 Karlovac
E-mail: mariokolar8@gmail.com

Prof. Pero RAOS, PhD
University of Slavonski Brod,
Mechanical Engineering Faculty in Slavonski Brod,
Trg Ivane Brlić Mažuranić 2, 35000 Slavonski Brod
E-mail: praos@unisb.hr

Hrvoje MEŠTRIĆ, PhD
Ministry of Science, Education and Youth of the Republic of Croatia,
Donje Svetice 38, 10000 Zagreb
E-mail: hmestric@gmail.com